Earthquake Geotechnical Engineering for Protection and Development of Environment and Constructions – Silvestri & Moraci (Eds)
© 2019 Associazione Geotecnica Italiana, Rome, Italy, ISBN 978-0-367-14328-2

Dynamic response of anchored retaining walls on a compliant foundation

C. Koutsantonakis
Department of Civil Engineering, University of Patras, Patras, Greece

G. Mylonakis
Department of Civil Engineering, University of Bristol, Bristol, UK University of Patras, Patras, Greece UCLA, Los Angeles, CA, USA

S.J. Brandenberg & J.P. Stewart
Department of Civil and Environmental Engineering, University of California at Los Angeles, Los Angeles, CA, USA

ABSTRACT: A simplified analytical solution is derived for the dynamic response of a flexible retaining wall constrained by a cable anchor installed at an arbitrary elevation along its height. The wall retains a linear viscoelastic homogeneous backfill of constant properties on a compliant foundation soil, and is excited by vertically-propagating harmonic S-waves under plane strain conditions. The simplifying assumptions of zero dynamic vertical normal stresses in the backfill and zero variation of vertical displacements with horizontal distance from the wall, originally adopted by Matsuo & Ohara 1960 and by Veletsos & Younan 1994, are employed. A closed-form solution based on a modified *Vlasov-Leontiev* formulation is derived, and an extensive parametric investigation is performed for exploring the effect of wall-soil interaction on seismic response. Simple expressions are obtained for wall deflections, soil thrusts, anchor and base shear forces, and base moments. The ratio of shear modulus between foundation and backfill controls the response of the system in conjunction with soil-wall relative stiffness. Results elucidate the importance of kinematic constraints on wall response. These aspects cannot be captured by conventional design methods based on limit state analysis which neglect kinematics and soil-structure interaction.

1 INTRODUCTION

Anchored retaining walls are widely used in deep excavations for lowering wall deflections and increasing the factor of safety against gravity loads. Despite their extensive use in practice, the effect of anchors on dynamic response remains poorly understood. Neelakantan et al. (1992) were among the first to assess soil pressures considering anchor forces in the framework of traditional limit-state methods (Okabe 1924, Mononobe and Matsuo 1929, Seed & Whitman 1970, Mylonakis et al 2007).

A number of numerical investigations of anchored retaining walls by means of the Finite-Element (FE) method were carried out by different investigators (Totsev 2006, Gazetas et al. 2016). Notwithstanding the importance of rigorous numerical solutions in providing insight into the physics of the problem, these methods are not ideal for routine use by engineers, given the sensitivity to often poorly defined input parameters and the computational effort required to explore a wide range of design parameters.

In this paper, a simplified analytical solution is developed, providing a mathematical framework for understanding and characterizing the dynamic response of flexible anchored walls retaining a homogeneous viscoelastic backfill resting on a compliant foundation soil. This method combines earlier proposals by Veletsos & Younan (1994), Li (1999), Kloukinas et al.

(2012) and Koutsantonakis et al. (2018). It is also inherently linked to the methods recently proposed by Brandenberg et al (2015, 2017a,b) and Durante et al (2019).

2 STATEMENT OF PROBLEM

2.1 *Equation of motion for the soil medium*

The problem under consideration is shown in Figure 1a, where a Cartesian coordinate system (x, y) is employed. A viscoelastic flexural wall of height H, thickness t_w, bending stiffness EI, mass density ρ_w, Poisson's ratio v_w and damping coefficient δ_w, retains a semi-infinite homogeneous soil stratum of constant thickness H, mass density ρ, *Poisson*'s ratio v, shear modulus G and damping coefficient δ. Both backfill and wall rest on a compliant foundation associated with a linear viscoelastic soil material of constant density ρ_f, shear modulus G_f and hysteretic damping coefficient δ_f. The wall is constrained by an elastic anchor placed at a height H_a from the base. The anchor is simulated as a linear elastic spring of constant stiffness K. The solution is developed in the frequency domain considering a harmonic base motion of constant frequency ω and amplitude $\ddot{X}_{gg}$ at the foundation soil – backfill interface, which leads to vertical S-wave propagation through the foundation soil and backfill.

To determine the response of the backfill, the method of separation of variables is employed:

$$u(x,y) = X(x)\ \Phi(y) \tag{1}$$

where $u = u(x, y)$ is the total horizontal soil displacement, $X(x)$ is an unknown function having dimensions of length, and $\Phi(y)$ is a known, in the finite-element sense, dimensionless function of depth.

Considering the equilibrium of horizontal forces acting on an arbitrary soil element in the retained soil medium and applying the assumptions of zero dynamic vertical normal stresses and zero variation of vertical displacement with the horizontal spatial coordinate (Matsuo & Ohara 1960, Veletsos & Younan 1994), the weak form of the equilibrium equation is obtained in terms of the differential equation:

$$\frac{d^2X(x)}{dx^2} - \left(\frac{\mathrm{a}_{oc}^2 - \mathrm{a}_o^2 + c_{oc}}{H^2\psi_e^2}\right)X(x) = \frac{\mathcal{L}\ddot{X}_g}{(V_S\psi_e)^2} \tag{2}$$

where,

$$\mathrm{a}_o = \omega \mathrm{H}/V_s^*;\ \mathrm{a}_{oc}^2 = H^2\int_0^H \Phi'(y)^2dy/\int_0^H \Phi(y)^2dy;\ c_{oc} = H^2\Phi(0)\Phi'(0)/\int_0^H \Phi(y)^2dy; \tag{3a, b, c}$$

$$L = \int_0^H \Phi(y)dy/\int_0^H \Phi(y)^2dy;\ \psi_e^2 = (2-\nu)/(1-\nu) \tag{4a, b}$$

Of the above parameters, a_o and a_{oc} denote a dimensionless excitation frequency and a cut-off frequency beyond which stress waves start to propagate horizontally in the backfill, respectively, while c_{oc} is a parameter associated with the non-zero horizontal displacement at the base of the backfill. $\mathcal{L}$ is a modal participation coefficient, $V_s^{*2} = G^*/\rho$ is the complex wave propagation velocity in the backfill, and ψ_e is a pertinent compressibility coefficient. $G^* = G\,(1+2i\delta)$ is the complex soil shear modulus. The validity of the associated simplifying assumptions of Matsuo & Ohara 1960 and Veletsos & Younan 1994 has been verified by Papazafeiropoulos & Psarropoulos 2010 by means of an exact analytical solution. Also, contrary to formulations pertaining to rigid rock conditions (Kloukinas et al 2012, Brandenberg et al 2017b), the derivative of the shape function Φ' appears outside the integral sign in parameter c_{oc} (Equation 3a).

The general solution to Equation 2 is:

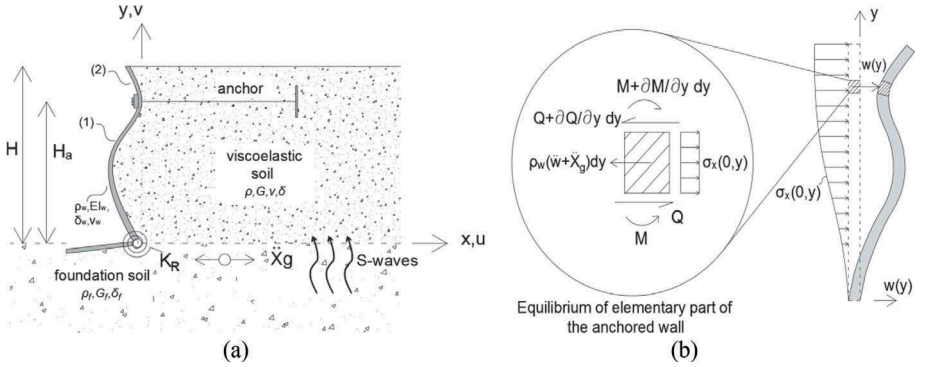

Figure 1. (a) System of an anchored flexible retaining wall and retained soil on a viscoelastic base stratum; (b) Equilibrium of forces on the wall.

$$X(x) = A_1 e^{mx} + A_2 e^{-mx} - \frac{\mathcal{L}\ddot{X}_g}{a_{oc}^2 - a_o^2 + c_{oc}} \left(\frac{H}{V_s^*}\right)^2 \tag{5}$$

where $m = \sqrt{a_{oc}^2 - a_o^2 + c_{oc}}/(H\psi_e)$ is a complex wavenumber associated with horizontally propagating waves. Determining the integration constants A_1 and A_2 requires imposing the following boundary conditions (Koutsantonakis et al. 2018):

$$u(x \to \infty, y) = u_{ff}(y); \quad u(0, y) = w(y) \tag{6a, b}$$

where $u_{ff}(y)$ is the free-field soil displacement at an infinite distance from the wall, and $w(y)$ is the deflection of the wall, at elevation y. To ensure finite response at large distances from the wall, integration constant A_1 must vanish. To determine $u_{ff}(y)$, the shape function $\Phi(y)$ can be taken equal to the fundamental natural mode shape of a homogeneous soil stratum on a flexible foundation (see Section 2.2 below). The associated soil thrusts are obtained in a straightforward manner from the easy-to-derive expression (Kloukinas et al. 2012):

$$\sigma_x(0, y) = \left(\frac{2}{1-\nu}\right) G^* \left.\frac{dX(x)}{dx}\right|_{x=0} \Phi(y) \tag{7}$$

2.2 *Fundamental shape function of backfill*

To determine the fundamental shape function of the retained soil layer, the one-dimensional wave function of Li (1999) is employed:

$$u(y) = A_3 \cos(k\ y) + A_4 \sin(k\ y) \tag{8}$$

where k is a wavenumber to be obtained as an eigenvalue; A_3 and A_4 are integration constants associated with the following boundary conditions:

$$\frac{\partial u(y=H)}{\partial y} = 0; \quad \frac{\partial^2 u(y=0)}{\partial y^2} = \left[i \left(\frac{\omega}{V_{sf}^*}\right) \left(\frac{\rho}{\rho_f}\right) \right] \frac{\partial u(y=0)}{\partial y} \tag{9a, b}$$

Equation 9b stands for the displacement compatibility and shear stress continuity at the base of the retained soil layer, where (ω/V_{sf}^*) is the wave number of the foundation soil layer. Combining Equations 8 and 9 yields the following characteristic equation for the eigenvalues k:

$$\cos(kH) + \left[i\left(\frac{V_s^*}{V_{sf}^*}\right)\left(\frac{\rho}{\rho_f}\right)\right]\sin(k\mathrm{H}) = 0 \tag{10}$$

which can be solved analytically for the complex fundamental eigenvalue, k_1. The corresponding shape function is complex valued, due to the effect of radiation and material damping, and is given by:

$$\phi(y) = \sin(k_1 y) - \left[i\left(\frac{\mathrm{a}_o}{\mathrm{a}_{o1}}\right)\left(\frac{V_s^*}{V_{sf}^*}\right)\left(\frac{\rho}{\rho_f}\right)\right]\cos(k_1 y) \tag{11}$$

2.3 *Equation of motion for the wall*

The retaining wall is modelled as an *Euler-Bernoulli* plate of unit width, as depicted in Figure 1b. Considering the equilibrium of horizontal forces acting at an arbitrary segment of the wall (Figure 1b) and employing Equation 7, the following governing equation is obtained:

$$EI^* w^{(4)}(y) + \left(\frac{2}{1-\nu} G^* m - \omega^2 \rho_w\right) w(y) = \left(\omega^2 \rho_w - \frac{2}{1-\nu}\frac{\mathcal{L} H^2 \rho m \Phi(y)}{\mathrm{a}_{oc}^2 - \mathrm{a}_o^2 + c_{oc}}\right)\ddot{X}_g \tag{12}$$

where $w(y)$ denotes the wall deflection, $EI^* = E_w^* \, t_w^3/[12\ (1t\ v_w^2)]$ and $E_w^* = E_w\ (1+2\ i\ \delta_w)$ denote the wall bending stiffness under plane strain conditions and the corresponding complex *Young's* modulus of the wall material, respectively. Equation 12 is a non-homogeneous, fourth-order ordinary differential equation, which can be solved in a straightforward manner once the function $\Phi(y)$ has been established.

3 PROPOSED SOLUTION

The general solution to Equation 12 can be derived and contains a number of integration constants that can be determined from the boundary conditions. It should be noticed that in the realm of the present analysis, the existence of the anchor does not affect the response of the free-field soil away from the wall. On the other hand, the anchor strongly influences the response of the wall due to the relative wall-soil displacements. The wall deflection is expressed in modular form as

$$w_1(y) = C_1\cos(\beta y) + C_2\sin(\beta y) + C_3\cosh(\beta y) + C_4\sinh(\beta y) + \frac{\rho_w \ddot{X}_g}{4\beta^4 EI^*} + \Lambda\Phi(y) \tag{13}$$

$$w_2(y) = C_5\cos(\beta y) + C_6\sin(\beta y) + C_7\cosh(\beta y) + C_8\sinh(\beta y) + \frac{\rho_w \ddot{X}_g}{4\beta^4 EI*} + \Lambda\Phi(y) \tag{14}$$

where, $\beta^4 = \left[2/(1-v)G*m - \omega^2\rho_w\right]/4EI*$ *and* $\Lambda = LH^2 m\ddot{X}_g\rho/\left[\left(a_o^2 - a_{oc}^2 - c_{oc}\right)(1-v)2E\ I*\left(\beta^4 + k_1^4\right)\right]$. Note that Equation (13) holds for $y < H_a$ (below anchor), and Equation (14) holds for $y \geq H_a$.

The integration constants C_1, C_2, C_3, C_4, C_5, C_6, C_7, C_8 are determined by enforcing the following boundary conditions at elevations $y = 0$ (base), $y = H_a$ (anchor level), and $y = H$ (top) of the wall:

$$w_1(0) = u(0);\ EI^* w_1^{(2)}(0) = K_R w_1^{(1)}(0) \tag{15a, b}$$

$$w_1(H_a) = w_2(H_a);\ w_1^{(1)}(H_a) = w_2^{(1)}(H_a); w_1^{(2)}(H_a) = w_2^{(2)}(H_a) \tag{15c, d, e}$$

$$w_1^{(3)}(H_a) = w_2^{(3)}(H_a) + K/EI^*[w_2(H_a) - w_1(0)] \tag{15f}$$

$$w_2^{(2)}(H) = 0;\ w_2^{(3)}(H) = 0 \tag{15g, h}$$

which pertain, respectively, to the equilibrium of shear stresses and moments at the base of the backfill, the boundary conditions at the anchor elevation H_a (compatibility of deflections and curvatures, equilibrium of bending moments and shear forces), and the boundary conditions of zero shear forces and moments at the top of the wall (Ghayesh 2012). Please note that the first of Equations 15a is tantamount to Equation 6b and naturally leads to a trivial result, so Equation 9b is used instead. K_R stands for the rotational stiffness of the wall foundation under plane strain conditions (Mushkelishvili 1954). It is stressed that in a more rigorous approach the anchor might undertake a portion of the total moment. In such a case, the anchor rotational stiffness must be included in the equilibrium of moments, but the specific effect is neglected here.

The dynamic soil thrusts are given by Equation 7 as:

$$\sigma_{x1}(0,y) = -\frac{2}{1-\nu}G^{*}m\left(\frac{\mathcal{L}\ddot{X}_g\Phi(y)}{\mathrm{a}_{oc}^2-\mathrm{a}_o^2+c_{oc}}\left(\frac{H}{V_s^{*}}\right)^2+w_1(y)\right), y<H_a \tag{16}$$

$$\sigma_{x2}(0,y) = -\frac{2}{1-\nu}G^{*}m\left(\frac{\mathcal{L}\ddot{X}_g\Phi(y)}{\mathrm{a}_{oc}^2-\mathrm{a}_o^2+c_{oc}}\left(\frac{H}{V_s^{*}}\right)^2+w_2(y)\right), yH_a \tag{17}$$

Based on the above analysis, the total base shear force Q_b and the base moment M_b of the wall can be obtained by integrating the soil thrusts along the wall height, taking into account the anchor force $Q_k = K\,[w_2(H_a)\ t\ w_1(0)]$. This leads to the expressions:

$$\sigma_b(0,y) = -\frac{2}{1-\nu}G^{*}m\left[\frac{\mathcal{L}\ddot{X}_g\Phi(y)}{\mathrm{a}_{oc}^2-\mathrm{a}_o^2+c_{oc}}\left(\frac{H}{V_s^{*}}\right)^2\int_0^H\Phi(y)dy+\int_0^{H_a}w_1(y)dy+\int_{H_a}^{H}w_2(y)\right] - K(w_2(H_a)-w_1(0)) \tag{18}$$

$$M_b = -\left(\frac{2}{1-\nu}\right)G^{*}m\left[\frac{\ddot{X}_g}{\mathrm{a}_{oc}^2-\mathrm{a}_o^2+c_{oc}}\left(\frac{H}{V_s^{*}}\right)^2\int_0^H y\Phi(y)dy+\int_0^{H_a}yw_1(y)dy+\int_{H_a}^{H}yw_2(y)dy\right] - KH_a(w_2(H_a)-w_1(0)) \tag{19}$$

For a better interpretation of the solution, the normalized flexibility $d_w = GH^3/EI^{*}$, normalized rotation compliance $d_\theta = GH^2/K_R$, normalized anchor cable stiffness $d_k = GH/K$, and normalized excitation frequency ω/ω_1 (ω_1 being the fundamental natural frequency of the retained soil mass), are introduced as the main independent variables (similar to Younan & Veletsos 2000).

4 PARAMETRIC INVESTIGATION

An extensive parametric investigation was carried out for the effects of flexible foundation, anchor and wall flexibility. In addition to the aforementioned dimensionless ratios d_w, d_θ, d_k and ω/ω_1, the following parameters were considered: $\nu = 1/3$, $\delta = \delta_f = 10\%$, $\delta_w = 4\%$ and $\rho_f/\rho = 1.3$.

4.1 *Influence of compliant foundation*

For the pseudo-static case ($\omega = 0$) the fundamental shape function $\Phi(y)$ takes the form of a sinusoidal function and is not affected significantly by the ratio (V_s/V_{sf}). Figure 2a presents the dynamic soil pressures at resonance. Note that the fundamental frequency depends on the ratio (V_s/V_{sf}), thus the fundamental frequency is different in each case examined ($V_{sf}/V_s = 1$, 3 and 5).

Note that wall flexibility in Figure 2 does not significantly affect the distribution of soil thrusts, as the curves for different values of d_w almost coincide. Nevertheless, a stiffening of the foundation ($V_{sf}/V_s = 1$ to 5) leads to an increase in normal stresses at all frequencies. Furthermore, a stiffer base attracts higher stresses. It should be noticed that the compliance of

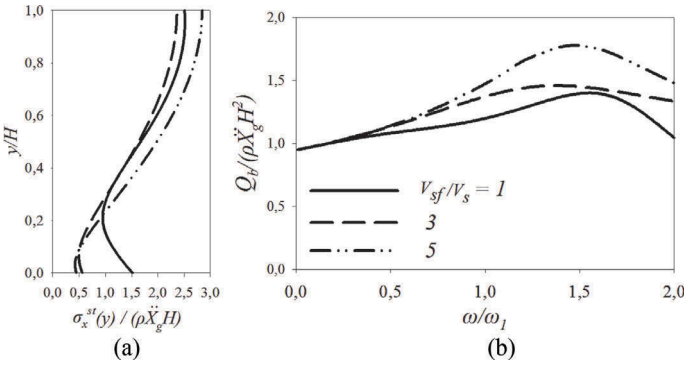

Figure 2. (a) Normalized soil pressures against normalized depth at resonance; (b) Normalized base shear force against normalized excitation frequency; $d_k \rightarrow \infty$, $d_\theta = 0$, $\rho_w = 0$.

foundation soil under the wall and the backfill is neglected in "bathtub" solutions involving a rigid base (Kloukinas et al. 2012; Brandenberg et al. 2017a, Koutsantonakis et al. 2018).

Integrating soil pressures with height, the total base shear force is obtained by means of Equation 18. Figure 2b depicts the normalized base shear force against excitation frequency. To provide a common reference for all plotted results, ω_1 in the abscissa of Figure 2b corresponds to a rigid base (i.e. $\omega_1 = \pi V_s / 2H$; $V_{sf}/V_s \rightarrow \infty$). For most applications the dominant energy from the input motions corresponds to $\omega/\omega_1 \ll 1$ which defines the most important range in the plot and highlights how significant it is to consider frequency effects in the particular problem. Evidently, foundation flexibility reduces significantly the base shear force even for small (V_{sf}/V_s) ratios. The reduction between the cases for $V_{sf}/V_s = 1$ and 5 is close to 30% at resonance. Also, a more flexible foundation (considering the variation in ρ_f/ρ values) leads to a more compliant system, thus the fundamental period increases, therefore reducing the seismic load imposed on the wall.

4.2 *Influence of anchor position and stiffness*

4.2.1 *Pseudostatic response*

The results presented below correspond to pseudo-static response ($\omega = 0$), fixed-base conditions ($d_\theta = 0$), rigid base ($V_{sf}/V_s \rightarrow \infty$), two values of normalized wall flexibility ($d_w = 10$ and 20), three values of anchor's cable stiffness ($d_k = 0.01$, 0.1 and 0.5) and two values of anchor height ($H_a/H = 0.7$ and 0.8). Note that d_w usually varies between 1 and 30 for most walls, and d_k varies between 0 and 1. Comparisons are presented against a numerical FE solution using Plaxis 2D, where a perfectly bonded soil-wall interface is assumed.

Figure 3a, b depict the variability of wall deformations, relative to the rigid base, against normalized height for different wall flexibilities d_w and anchor stiffness d_k. The main influence for wall deflections is the anchor location. High values of H_a/H ratio lead to small wall displacements. Also, for low anchor stiffness the influence of wall flexibility decreases significantly and the wall deflection atop the wall drops by as much as 80%.

The distribution of contact pressures (Figure 3c,d) is less affected by wall flexibility, but strongly correlates to anchor stiffness. As dynamic soil stresses are related to relative wall-free field displacements, a softer cable tends to produce lower relative-to-the-free-field wall displacements and, therefore, lower soil thrusts (up to about 40% for $H_a/H = 0.7$ and 25% for $H_a/H = 0.8$). For high H_a/H ratios, stiff cables and flexible walls, the distribution of contact pressures is almost linear with height. Generally speaking, wall flexibility (d_w) affects the thrust distribution near the top of the wall for low values of ratio of H_a/H, and near the middle of the wall for high values of H_a/H.

The results in Figures 3 and 4 suggest a good agreement between the predictions of the proposed solution and the numerical results by Plaxis 2D, both in terms of wall deflections and wall pressures. Note that the total shear force Q_{tot} is obtained by integrating the soil pressures,

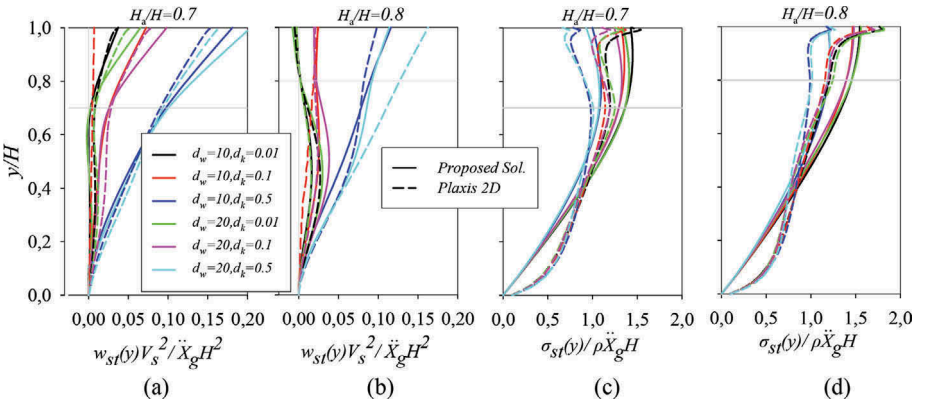

Figure 3. Normalized pseudo-static (a), (b) wall deflection and (c), (d) soil pressure against normalized depth for a fixed-base, anchored flexible wall; $\rho_w = 0$.

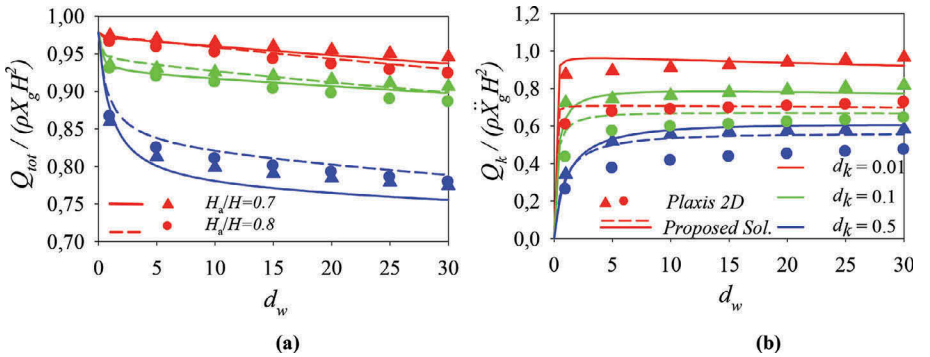

Figure 4. Normalized (a) total shear, (b) anchor shear force against wall flexibility d_w for pseudo-static conditions; $\rho_w = 0$.

the anchor shear force is $Q_k = K\,[w_2(H_a)\ t\ w_1(0)]$ and the base shear force is then obtained as the difference between Q_{tot} and Q_k.

Figure 4 depicts the variation of Q_{tot} and Q_k with wall flexibility d_w. Evidently, increasing wall flexibility decreases the total amount of shear force while the anchor shear force remains steady. Thus, increasing d_w the base shear force decreases. Also, increasing the anchor stiffness d_k, the deviation between the proposed solution and the FE results increases.

4.2.2 *Dynamic response*

The influence of frequency on the dynamic response of the system is shown in Figure 5 in terms of normalized base shear Q_b and anchor shear force Q_k.

As shown in Figure 5, the anchor undertakes a strong portion of the dynamic thrust (over 50%) and, as already discussed, provides an important kinematic constraint on the wall. For stiffer cables (lower d_k values), a higher percentage of the total shear force is carried by the anchor (higher Q_k) and a lower force is imposed on the foundation (lower Q_b). The elevation of the anchor is important as an increase in H_a/H from 0.7 to 0.8 leads to a 30% reduction in anchor force and a 60% increment in base shear (Figure 4).

As shown in Figure 5, wall flexibility strongly affects the base shear only near resonance regardless of H_a/H and anchor stiffness d_k. The maximum reduction (Q_k) or increment (Q_b) for $\omega/\omega_1 \neq 1$ as a result of wall flexibility, is lower than 20%. Note that contrary to the compliance of foundation soil, the anchor and the wall do not affect the fundamental frequency of the system.

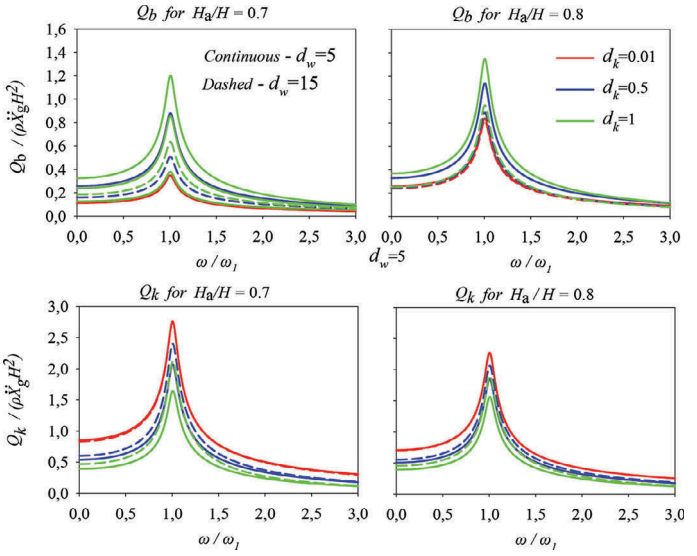

Figure 5. Normalized dynamic anchor shear and base shear force against normalized excitation frequency for a fixed-base wall; continuous line for d_w=5 and dashed for d_w =15.

5 CONCLUSIONS

A simplified analytical solution was developed to assess the dynamic response of flexible retaining walls with anchors resting on a compliant soil. The results of a parametric investigation indicate that the stiffness of foundation soil relative to the backfill (expressed through the ratio V_{sf}/V_s) has a profound effect on the response, by limiting the influence of wall flexibility and anchor stiffness. By varying this parameter it was found that a stiff foundation soil (accounting for the ρ_f/ρ ratio) generates higher dynamic loads and also increases the fundamental natural frequency of the system relative to a softer one. For a compliant foundation soil, anchor elevation and stiffness strongly affect the response of the system by limiting wall displacements and soil pressures. Anchor elevation H_a/H influences mainly wall displacements and curvatures. Moreover, wall flexibility leads to lower dynamic thrusts in combination with anchor elevation and stiffness. As a final remark, it should be reiterated that the above essential parameters are neglected by limit state methods, such as the Mononobe-Okabe formulae and their variants, the use of which should gradually be discontinued.

REFERENCES

Brandenberg, S.J., Stewart, J.P. & Mylonakis, G. 2017a. Influence of wall flexibility on seismic earth pressures in vertically homogeneous soil. *Proc. Geo-Risk 2017: Impact of spatial variability, Probabilistic site characterization and geohazards*. Geotechnical special publication No 285. Denver. CO.

Brandenberg, S.J., Mylonakis, G. & Stewart, J.P. 2017b. Approximate solution for seismic earth pressures on rigid walls retaining inhomogeneous elastic soil. *Soil Dynamics and Earthquake Eng* 97: 468-477.

Brandenberg, S.J., Mylonakis, G.M Stewart, J.P., 2015. Kinematic Framework for Evaluating Seismic Earth Pressures on Retaining Walls, *J. Geotech & Geo-Environmental Engineering*, ASCE, 141, 7

Durante, M.G., Brandenberg, S.J., Dashti, S., Stewart, J.P., Mylonakis, G. 2019. Analysis of seismic earth pressures on flexible underground box structures. *Proc. of 7th International conference on earthquake geotechnical engineering, 17-20 June*. Roma. Italy (under review).

Gazetas, G., Garini, E. & Zafeirakos, A. 2016. Seismic analysis of tall anchored sheet-pile walls. *Soil Dynamics and Earthquake Engineering* 91: 209-221.

Ghayesh, M. 2012. Nonlinear dynamic response of a simply-supported Kelvin-Voigt viscoelastic beam, additionally supported by a nonlinear spring. *Nonlinear analysis: Real world appls* 13: 1319-1333.

Kloukinas, P., Langousis, M. & Mylonakis, G. 2012. Simple wave solution for seismic earth pressures on nonyielding walls. *Geotechnical and Geonenvironmental Engineering* 138: 1514-1519.

Koutsantonakis, C., Mylonakis, G., Brandenberg, S.J., Durante, M. & Stewart, J.P. 2018. Seismic response of flexible walls retaining homogeneous viscoelastic soil. *Proc. of 16th European conference on earthquake engineering, 18-22 June*. Thessaloniki. Greece.

Li, X. 1999. Dynamic analysis of rigid walls considering flexible foundation. *Geotechnical and Geoenvironmental Engineering* 125: 803-806.

Matsuo, H. & Ohara, S. (1960). Lateral earth pressures and stability of quay walls during earthquakes. *Proc. of 2nd World engineering congress, 29 October – 7 November*, Tokyo, Japan.

Mononobe, N. & Matsuo, M. 1929. On the determination of earth pressures during earthquakes. *Proc. of 2nd World engineering congress, 29 October – 7 November*, Tokyo. Japan.

Muskhelishvili, N. 1954. Some basic problems of the mathematical theory of elasticity. 4th ed. Moscow: Springer – science and business media.

Mylonakis, G., Kloukinas, P., Papantonopoulos, C. 2007. An alternative to the Mononobe–Okabe equations for seismic earth pressures. *Soil Dynamics and Earthquake Engineering*; 27: 957-969.

Neelakantan, G., Budhu, M. & Richards, R. 1992. Balanced seismic design of anchored retaining walls. *Geotechnical Engineering* 118: 873-888.

Okabe, S. 1924. General theory on earth pressure and seismic stability of retaining wall and dam. *Japanese society of civil engineering* 12: 34-41.

Papazafeiropoulos, G. & Psarropoulos, P. 2010. Analytical evaluation of the dynamic distress of rigid fixed-base retaining systems. *Soil Dynamics and Earthquake Engineering* 30: 1446-1461.

Totsev, A. 2006. Numerical analysis of anchored diaphragm walls (relationship between FEM and SRM), University of ACEG. Sofia.

Veletsos, A.S. & Younan, A. 1994. Dynamic soil pressures on rigid vertical walls. *Earthquake Engineering and Structural Dynamics* 23: 275-301.

Vrettos C., Beskos D.E., Triantafyllidis T. 2016. Seismic pressures on rigid cantilever walls retaining elastic continuously non-homogeneous soil: An exact solution. *Soil Dynamics and Earthquake Engineering*; 82, 142-153.

Younan A.H., Veletsos A.S. 2000. Dynamic response of flexible retaining walls. *Earthquake Engineering and Structural Dynamics* 29: 1815-1844.